

Surface core-level shifts for Pt single-crystal surfaces

R. C. Baetzold, G. Apai, and E. Shustorovich

Research Laboratories, Eastman Kodak Company, Rochester, New York 14650

R. Jaeger

Stanford Synchrotron Radiation Laboratory, Stanford University, Stanford, California 94305

(Received 8 February 1982; revised manuscript received 21 February 1982)

The (111) and (110) surfaces of Pt, clean, oxidized, and covered by CO, have been investigated for surface $4f$ core-level binding-energy shifts. For the (111) face the surface Pt $4f_{7/2}$ core level was shifted by 0.40 ± 0.05 eV to lower binding energy relative to the bulk peak. On the (110)-(1 \times 2) reconstructed surface similarly shifted peaks at 0.21 ± 0.05 and 0.55 ± 0.05 eV were observed. Chemisorbed carbon monoxide shifts the Pt(111) surface-related core level by 1.3 eV to higher binding energy. Formation of subsurface oxygen did not produce changes in the Pt(111) $4f_{7/2}$ core-level binding energies. The results obtained are explained and their possible implications are discussed.

I. INTRODUCTION

The understanding of how charge is distributed between surface and bulk regions of a metal as well as between adsorbates and the metal substrate is of crucial importance for a meaningful description of surface-related processes. Recent photoemission experiments have demonstrated that surface-induced core binding energy (CBE) shifts can be detected on $5d$ transition metals [Au (Ref. 1), W (Ref. 2), Ir (Ref. 3), and Ta (Ref. 4)]. Furthermore, in some of these experiments the energy separation between the bulk and surface $4f$ core levels has been shown to be sensitive to structural details of the surface. van der Veen *et al.*,³ for example, have found that the shift observed in the $4f$ level of the surface atoms and the intensity of this peak relative to that observed from the bulk atoms of Ir single crystals correlate with crystallographic orientation and reconstruction of the surface. These findings were also confirmed for Au surfaces.⁵ The presence of energetically different core levels of surface and bulk atoms of the substrate allows, in principle, the measurement of relative changes in electronic structure as well as coordination numbers for the surface atoms due to chemisorption or reconstruction. This ability to monitor surface and bulk electronic structures separately should have a considerable effect on future catalysis studies. It is therefore important to extend such studies to all transition metals.

Here we report the results of the first stage of a systematic study⁶ of surface $4f$ shifts for clean and

adsorbate-covered high-density (HD) flat surfaces and low-density (LD) stepped surfaces of platinum, a metal of great catalytic importance. We observe a surface CBE shift of ~ 0.4 eV to lower binding energy for the clean (111) surface and two shifts, one of ~ 0.55 eV and another of ~ 0.21 eV, to lower binding energy for the (110) surface of platinum. This indicates that the (110)-(1 \times 2) surface of Pt is composed of two types of coordination sites, in contrast to the Pt(111) surface. We have also investigated the influence of chemisorbed electron-withdrawing adsorbates on the surface $4f_{7/2}$ core levels of Pt(111) and studied the high-temperature "oxide" state of Pt(111) by comparing the $4f_{7/2}$ and valence-band photoemission spectra.

II. EXPERIMENTAL

Experiments were performed in an ion- and Ti-pumped ultrahigh-vacuum chamber (base pressure $\sim 2 \times 10^{-10}$ Torr) connected to the grasshopper monochromator (recoated 1200 lines/mm holographic grating) on beam line I-1 at the Stanford Synchrotron Radiation Laboratory under parasitic beam conditions.

The Pt $4f$ core-level photoemission spectra were recorded at $h\nu = 150$ eV (angle of incidence $\sim 30^\circ$, p polarization) with a double-pass cylindrical-mirror analyzer (CMA) operated with the narrow aperture at a pass energy of 10 eV. Our combined instrumental resolution (monochromator plus analyzer)

was 0.35 eV.

Auger-electron spectroscopy (AES), soft-x-ray photoelectron spectroscopy (PES), and soft-x-ray absorption-edge measurements were used to determine surface cleanliness and to characterize the adsorbate layers. PES of the valence-band (VB) region at $h\nu=170$ eV was particularly useful for this purpose. By choosing the photon energy so that the cross section for the $5d$ states of Pt is low (at the Cooper minimum), we easily detected molecular orbital contributions of adsorbates.

The Pt single-crystal disks (~ 1 -mm thick) were cut by spark erosion from an Atomergic Chemetals Company single-crystal rod (99.999% purity) after orientation by Laue diffraction. The disks were polished, rechecked for alignment, and mounted on a molybdenum block that allowed indirect heating up to 1300 K. Clean surfaces were prepared after many cycles of *in situ* chemical cleaning and argon-ion sputtering at various temperatures. The chemical cleaning consisted of exposing the crystal to NO at high temperatures. This treatment removed the main contaminant, carbon, as well as trace sulfur impurities. Any remaining oxygen was removed by flashing the crystals to high temperature in ultrahigh vacuum. Ion sputtering reduced the AES peaks of contaminants [P (120 eV), Ca (291 eV)] to below 3% of the Pt (237-eV) peak. The samples were checked for Si contamination in photoemission. The clean, annealed surfaces were also characterized by low-energy electron diffraction (LEED). The Pt(110) surface showed the (1×2) reconstruction pattern.

III. RESULTS AND DISCUSSION

A. Clean surfaces

The $4f_{7/2}$ core-level photoemission spectra ($h\nu=150$ eV) from the clean Pt(111) and Pt(110) samples are shown in Fig. 1. The binding energy of the $4f_{7/2}$ bulk levels relative to the Fermi energy is 71.1 ± 0.1 eV for both samples, which agrees with a recent compilation of x-ray photoelectron spectroscopy (XPS) core-level energies.⁷

Because Pt is a metal with a strongly modulated density of states near E_F , analysis of the $4f_{7/2}$ line shape was performed using an exponential function of the form $e^{-E/\zeta}/E^{1-\alpha}$, using ζ and α as adjustable parameters.⁸ This function was superimposed on a linear background of secondary electrons and convoluted with a slightly skewed Gaussian instrumental resolution function with a full width at half

maximum (FWHM) of 0.35 eV.⁹

For the Pt(111) sample, good agreement was found with the surface peak being shifted by 0.40 ± 0.05 eV toward lower binding energy—this shift being in good agreement with the shift predicted by Rosengren and Johansson.¹⁰ The ratio of the areas under the surface and bulk peaks is 1.1:1, respectively. For the Pt(110) crystal face the shift of the Pt $4f_{7/2}$ level for the surface atoms was about 0.21 ± 0.05 eV, which is less than the experimental resolution. However, a considerable tailing of the $4f_{7/2}$ photoemission at the low-binding-energy (BE) side could be fitted only with an additional surface peak shifted by about 0.55 eV toward lower binding energy relative to the bulk peak. The ratio of the areas of these two surface peaks is about 2:1 [$A(\Delta E=0.21$ eV)/ $A(\Delta E=0.55$ eV)]. It is a general idea, based upon theoretical^{10,11} and experimental¹⁻⁵ grounds, that less dense surfaces show larger surface shifts. Our results are consistent with this idea and show that the Pt(111) surface layer is substantially homogeneous (ideally, all surface atoms have 9 nearest neighbors compared to 12 for the bulk atoms), whereas the Pt(110) surface layer is a heterogeneous mixture of two sites with different environments (without reconstruction, the coordination numbers of surface atoms in the troughs and

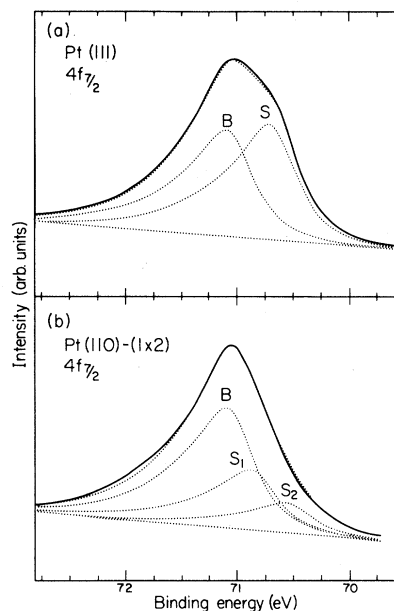


FIG. 1. Pt $4f_{7/2}$ photoemission from (a) the clean Pt(111) surface and (b) the Pt(110)- (1×2) surface. The thin solid lines represent the line-shape analysis, as discussed in the text. The linear secondary electron background is indicated. (B—bulk peak; S, S_1 , and S_2 —surface peaks.)

crests are 11 and 7, respectively). Indeed, site 1 (in the troughs) produces a surface shift of about 0.21 eV and can be interpreted as more "bulklike" than the surface sites on Pt(111). On the other hand, site 2 (in the crests), with a surface shift of about 0.55 eV, has a more open environment than the sites on the Pt(111) surface, which show bulk symmetry and a negligible change of the first interlayer spacing.¹²

Because the intensity ratio of the two Pt(110) peaks is near 2:1, surface reconstruction is revealed and one can discriminate between the various reconstruction models.^{13,14} Though fcc (110)-(1×2) reconstruction is well known in the published LEED literature for the (110) planes of Ir, Pt, and Au, some uncertainty remains as to the exact configuration of the surface atoms.¹³ Three models have been proposed: (1) the "missing row" model in which every other close-packed [110] row in the outermost layer is missing, (2) the "rumpled-buckled" model where every other [110] row is relaxed perpendicular to the crystal surface, and (3) the "planar-pairing" model in which every two adjacent rows of the first layer are paired to form one row. Dynamic LEED calculations for the Pt(110)-(1×2) surface in particular yield closest agreement for the missing-row model in which the spacing between the first and second layers is expanded by +23%.¹⁴ However, a second, shallower minimum in the plot of r factor versus first interlayer spacing is reported for a 20% contraction of the bulk value.¹⁴

The findings of this work support the missing-row model with the surface layer resulting in the formation of site 2 (in the crests). Site 1 (in the troughs) would be represented by the second-layer atoms. The surface shift of the $4f_{7/2}$ levels could be further decreased as opposed to the Pt(111) surface by a slight displacement of these atoms forming a planar pairing of the second layer. Also, a planar pairing of this kind slightly improved the r -factor analysis by Adams *et al.*¹⁴ An additional argument for the missing-row model is the relative occupation number of the two surface sites, N_1/N_2 , which we found to be close to 2:1. Whereas a buckled surface would result in a ratio of 1:1, the missing-row model is consistent with the ratio 2:1.

B. Chemisorption of carbon monoxide on the Pt(111) surface

The bonding of CO molecules to Pt surfaces is believed to involve the 5σ carbon lone-pair orbital and metal $5s6p$ electrons with backbonding from

the Pt $5d$ states into the unoccupied π^* orbital of CO, the backbonding appearing predominant.¹⁵ Since this proposed charge transfer is mainly from the localized d states, the surface core-level shifts should be sensitive to the Pt-CO bond.

Photoemission spectra of the valence band of Pt(111) exposed to ~ 15 -L CO (1 L=1 langmuir = 10^{-6} Torr sec) were taken at a photon energy of 170 eV and showed molecular levels indicative of molecularly adsorbed CO. Figure 2 shows the associated $4f_{7/2}$ core-level photoemission spectrum to be compared with the clean Pt(111) spectrum of Fig. 1. Upon chemisorption of CO there is an attenuation of the surface peak with an associated chemisorption-induced substrate peak shifted by about 1.3 eV to higher binding energy. The line-shape analysis described earlier was performed for the $4f_{7/2}$ peak of Fig. 2 and showed good agreement with the data when the CO-induced surface peak *C* had a larger FWHM (1.3 times) than the clean surface peak *S*, the ratio of the areas under peaks *C* and *S* being about 1:1. The CO-induced shift to higher binding energy is fully consistent with the electron-withdrawing nature of CO. Moreover, this shift is so large (ca. 1.3 eV) that the peak *C* is even higher in binding energy than the bulk peak (*B*). Similar shifts have also been observed for other electron-withdrawing adsorbates such as H in H-W(100) (Ref. 4) and H-Ir(111) (Ref. 3) and O in O-W(110).^{2,16} For the study of oxygen adsorbed on W(110) (Ref. 16), separate W $4f_{7/2}$ core-level shifts were attributed to the systems of isolated oxygen on W(110) and $p(2\times 1)$ oxygen islands on W(110). In this respect, our observation of only one CO-

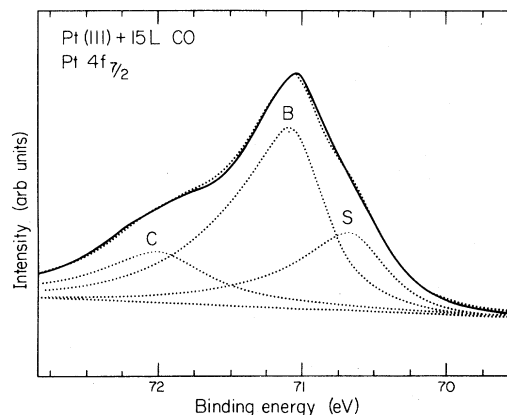


FIG. 2. Pt $4f_{7/2}$ photoemission from the Pt(111) surface after exposure to 15-L CO. The thin solid lines represent the line-shape analysis, as discussed in the text. (*B*—bulk peak; *S*—surface peak; *C*—surface with CO peak.)

induced peak of greater FWHM than the other core peaks can be understood in terms of different adsorption sites for CO. The presently accepted structure model of the saturation layer of CO on the Pt(111) surface describes the CO layer as a mixture of "on-top" and "bridge-site" CO molecules with the ratio of 1:1.¹⁷ Only the CO-induced peak is observed, probably because the difference in the $4f_{7/2}$ photoemission shift between "on-top" and "bridge-site" Pt-CO bonds is too small to be resolved in the present work. The rather broad CO-induced peak points also in this direction. At the same time, the existence of the residual peak *S* in Fig. 2, apparently due to surface atoms unaffected by the CO chemisorption, is puzzling. Indeed, how could the Pt(111) surface atoms remain unaffected under the ambient CO exposure of ≥ 15 L, which is usually claimed to be sufficient for saturation? The answer may be related to the fact that there can be a considerable (~ 15 – 20 %) concentration of chemisorbed CO at the ubiquitous imperfections (steps and kinks) of a real Pt(111) surface.¹⁸ If this is so, it is reasonable that some partially coordinated Pt atoms remain sterically inaccessible to the CO. We would also expect to find this behavior for CO chemisorption on Pt(110), since atoms in the troughs are sterically blocked by atoms in the crests. These points will be explored in our future experiments with stepped and kinked surfaces.

C. Interaction of oxygen with the Pt(111) sample: Chemisorption versus oxidation

Experimental evidence suggests that the interaction of oxygen and Pt at the Pt(111) surface results in two different states. The substrate temperature during the O_2 exposure determines which state forms. The "chemisorbed" or loosely bound state forms below 800 K, whereas the "oxide" or strongly bound state forms above 800 K.¹⁹

In the present study the chemisorbed state was produced by exposing the clean Pt(111) surface at room temperature to ~ 20 -L O_2 with 10^{-6} -Torr O_2 in the chamber. The oxide state was generated by exposing the hot Pt(111) surface ($\sim 900^\circ\text{C}$) to oxygen from a capillary doser (~ 1 -mm diameter) located directly in front of the crystal face. For both adsorption configurations the pressure was measured by a nude Bayard-Alpert gauge. The oxide state was formed at a pressure of 3×10^{-7} -Torr oxygen (uncorrected for the capillary doser) for about 15 min while the ion pump was (partly) throttled. Both states were characterized by their valence-

band photoemission spectra taken at $h\nu = 170$ eV, which clearly showed differences in the $O 2p$ and $O 2s$ contributions to the substrate photoemission. The major barrier to achieving a $4f_{7/2}$ photoemission spectrum of the chemisorbed state with good statistics and high resolution was the interaction of ambient CO with the adsorbed oxygen layer. We observed a removal of oxygen from the surface. Our data are, therefore, only preliminary. We found indication that the effects of chemisorbed oxygen on the $4f_{7/2}$ spectrum are analogous to those observed for CO (see Fig. 2). This observation needs further support by high-resolution studies at more intense photon flux.

The $4f_{7/2}$ spectrum of the oxide state is shown in Fig. 3. Quite surprisingly, it is almost identical with the spectrum obtained for the clean Pt(111) surface. We found good agreement to the line-shape fit with the same parameters as for the clean Pt(111) surface, as shown in Fig. 3. The surface peak has not diminished nor has the separation of bulk and surface peaks changed. The lack of change in the $4f_{7/2}$ photoemission from the oxide state shows that the surface must be similar to the clean (111) surface. The oxide detected in the valence region of the photoemission spectrum must be a subsurface form of oxygen. This agrees with other experiments.^{19–21} Ion-scattering data by Niehus and Comsa²¹ show that at least the first layer of an oxidized Pt(111) sample consists entirely of Pt atoms.

The constant $4f_{7/2}$ BE observed for the Pt bulk atoms suggests that the interaction of the incorporated oxygen atoms with the platinum bulk layers

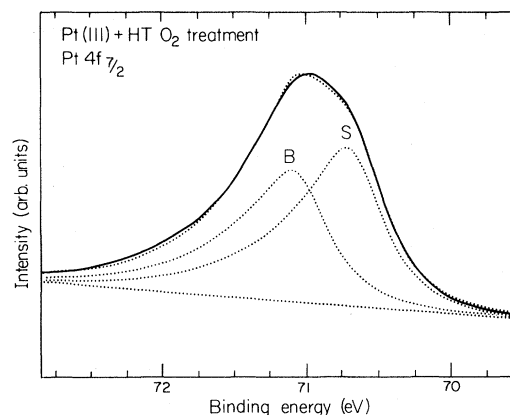


FIG. 3. Pt $4f_{7/2}$ photoemission from the oxidized Pt(111) sample. Note the similarity to the spectrum of the clean Pt(111) surface. The thin solid lines represent the line-shape analysis of the clean Pt(111) surface. (*B*—bulk peak; *S*—surface peak.)

may be quite different from what is expected for a formal platinum oxide species. A recent LEED and thermodynamic analysis²² of the oxygen-platinum system has concluded that after high-temperature treatment in oxygen a metastable solid solution of oxygen in platinum is formed upon cooling. This solid solution is disordered, although ordered phases can form by oxygen movement. The solid-solution observation is consistent with the lack of Pt surface core shift. An alternative explanation for this apparently weak interaction between the incorporated oxygen and its host would be a striking difference in the escape depth of the $4f_{7/2}$ and valence electrons due to their difference in final-state energies.²³ We cannot exclude that the $4f_{7/2}$ spectrum of the oxidized Pt(111) sample contains mainly photoelectrons of near-surface Pt atoms not involved in the subsurface oxide, whereas the photoelectrons emitted from the subsurface region are inelastically scattered out of the $4f_{7/2}$ photoemission energy range.

Finally, we want to comment briefly on recent studies²⁴ that emphasized that bulk-dissolved silicon may be responsible for the oxide formation on Pt(111) surfaces. These studies, using either Si-contaminated Pt crystals or evaporated Si on Pt surfaces, showed that the general characteristics of the Pt oxide state can be duplicated. Since we have not detected photoemission due to Si contaminations, we tend to rule out this explanation for the subsurface oxygen formation in our study.

IV. CONCLUSIONS

The Pt $4f_{7/2}$ core-level spectra are sensitive to the surface structure of Pt(111) and Pt(110)-(1×2). Whereas we observed a surface shift of 0.4 ± 0.05 eV toward lower BE on the Pt(111) surface, the surface shift of the major surface contribution on the Pt(110)-(1×2) surface is 0.21 eV with some evi-

dence for a second surface peak shifted by about 0.55 eV relative to the bulk peak. Studies of this kind can help discriminate between different reconstruction models of LEED calculations. The present result for the clean Pt(110)-(1×2) surface favors the missing-row model possibly accompanied by a planar pairing in the second layer.

Chemisorption of CO on the Pt(111) surface induces a surface-related chemical shift by about 1.3 eV toward higher BE (relative to the surface peak of the clean surface) attributable to Pt surface atoms that have transferred charge to chemisorbed CO molecules.

The interaction of oxygen with the Pt(111) sample above 800 K results in virtually no change of the $4f_{7/2}$ core-level position, whereas the valence-band photoemission clearly shows the presence of oxygen. These findings point to a subsurface oxygen species. By this we establish the promising potential of high-resolution substrate core-level photoemission studies at appropriate photon energies to discriminate surface and subsurface phenomena.

ACKNOWLEDGMENTS

We thank J. Stöhr for use of the UHV chamber, R. Treichler for help in the early phases of our experiments, and R. Morris for fabricating several parts of the equipment. We are grateful to Gabor Somorjai for valuable discussions and to Winifred Heppler and Gabor Somorjai for preparation of the crystal surfaces. We are grateful to Randall Mack for computer programming and fitting of the line shape in this work. One of us (R.J.) thanks Eberhard Umbach for valuable discussions and Eastman Kodak Company for financial support. This work was in part supported by the Stanford Synchrotron Radiation Laboratory under National Science Foundation funding.

¹P. H. Citrin, G. K. Wertheim, and Y. Baer, *Phys. Rev. Lett.* **41**, 1425 (1978).

²T. M. Duc, C. Guillot, Y. Lassailly, J. Lecante, Y. Jugnet, and J. C. Vedrine, *Phys. Rev. Lett.* **43**, 789 (1979).

³J. F. van der Veen, F. J. Himpsel, and D. E. Eastman, *Phys. Rev. Lett.* **44**, 189 (1980); **44**, 553(E) (1980).

⁴J. F. van der Veen, P. Heimann, F. J. Himpsel, and D. E. Eastman, *Solid State Commun.* **37**, 555 (1981).

⁵P. Heimann, J. F. van der Veen, and D. E. Eastman, *Solid State Commun.* **38**, 595 (1981).

⁶G. Apai, R. C. Baetzold, E. Shustorovich, and R.

Jaeger, *Surf. Sci. Lett.* **116**, L191 (1982).

⁷J. C. Fuggle and N. Martensson, *J. Electron Spectrosc. Relat. Phenom.* **21**, 275 (1980).

⁸G. D. Mahan, *Phys. Rev. B* **12**, 4814 (1975); G. K. Wertheim and L. R. Walker, *J. Phys. F* **6**, 2297 (1976); G. K. Wertheim and P. H. Citrin, *Top. Appl. Phys.* **26**, 197 (1978).

⁹In a previous Letter [*Surf. Sci.* **116**, L191 (1982)] line-shape analysis was performed using a Doniach-Šunjić function convoluted with a Gaussian instrumental function. The peak separations obtained by the two

methods agree within the experimental uncertainty; however, the Doniach-Šunjić function produces a poorer fit on the high-binding-energy side of the $4f_{7/2}$ peak. The need for the procedure used here to fit Pt line shapes was discussed in Ref. 8.

- ¹⁰A. Rosengren and B. Johansson, *Phys. Rev. B* **22**, 3706 (1980).
- ¹¹M. C. Desjonqueres, D. Spanjaard, Y. Lassailly, and C. Guillot, *Solid State Commun.* **34**, 807 (1980).
- ¹²J. F. van der Veen, R. G. Smeenk, R. M. Tromp, and F. W. Saris, *Surf. Sci.* **79**, 219 (1979), and references therein.
- ¹³M. Moritz and D. Wolf, *Surf. Sci.* **88**, L29 (1979); C.-M. Chan, M. A. van Hove, W. H. Weinberg, and E. D. Williams, *ibid.* **91**, 440 (1980).
- ¹⁴D. L. Adams, H. B. Nielsen, M. A. van Hove, and A. Ignatiev, *Surf. Sci.* **104**, 47 (1981).
- ¹⁵See, for instance, W. Andreoni and C. M. Varma, *Phys. Rev. B* **23**, 437 (1981), and references therein.
- ¹⁶G. Treglia, M. C. Desjonqueres, D. Spanjaard, Y. Lassailly, C. Guillot, Y. Jugnet, T. M. Duc, and J. Lecante, *J. Phys. C* **14**, 3463 (1981).
- ¹⁷H. Froitzheim, H. Hopster, H. Ibach, and S. Lehwald, *Appl. Phys.* **13**, 147 (1977); H. Hopster and H. Ibach, *Surf. Sci.* **77**, 109 (1978).
- ¹⁸C. M. Friend, R. M. Gavin, E. L. Muetterties, and M.-C. Tsai, *J. Am. Chem. Soc.* **102**, 1717 (1980), and references therein.
- ¹⁹R. Ducros and R. P. Merrill, *Surf. Sci.* **55**, 227 (1976); R. W. McCabe and L. D. Schmidt, *ibid.* **60**, 85 (1976); **65**, 189 (1972); C. E. Smith, J. P. Biberian, and G. A. Somorjai, *ibid.* **57**, 426 (1979).
- ²⁰J. L. Gland, B. A. Sexton, and G. B. Fisher, *Surf. Sci.* **95**, 587 (1980).
- ²¹H. Niehus and G. Comsa, *Surf. Sci.* **93**, L147 (1980).
- ²²M. Salmerón, L. Brewer, and G. Somorjai, *Surf. Sci.* **112**, 207 (1981).
- ²³Whereas the Pt $4f_{7/2}$ photoelectron had a kinetic energy of 74 eV ($h\nu=150$ eV), the oxygen $2p$ electrons were detected at ~ 142 eV kinetic energy ($h\nu=170$ eV). In principle, the effect of escape depth can be discriminated against other effects by taking both photoemission spectra at the same escape depth. Since the high adsorbate sensitivity of the valence spectrum can be maintained only at the Cooper minimum of the Pt $5d$ cross section, the $4f_{7/2}$ spectra would have to be taken at the photon energy, 220 eV. However, at this energy the resolution of the monochromator would be only ≥ 0.6 eV, which would prevent a direct comparison with the data taken at $h\nu=150$ eV.
- ²⁴H. Niehus and G. Comsa, *Surf. Sci.* **102**, L14 (1981); H. P. Bonzel, A. M. Franken, and G. Pirug, *ibid.* **104**, 625 (1981).